JOURNAL OF OPTOELECTRONICS AND ADVANCED MATERIALS, Vol. 12, No. 5, May 2010, p. 1000 - 1003

Kink-free L-I and low threshold current of violet InGaN laser diode due to optimization of the barrier thickness and type

R. A. ABDULLAH*, K. IBRAHIM
Nano-Optoelectronics Research and Technology Laboratory (N.O.R)
School of Physics, Universiti Sains Malaysia,11800 Penang, Malaysia

The effects of the barrier thickness and type on the threshold current and I-L curve shape of violet InGaN laser diode (LD) have numerically been investigated. The simulation result indicated that the thickness of the barrier layer plays an important role in determining the threshold current as well as the output power of the LD. The lowest threshold current has been obtained with the lowest barrier thickness, exactly equal to 4 nm. On the other hand, simulation result indicated that the thinner barrier leads to the appearance of the kink in I-L curve due to increase in the polarization at the barriers/wells interfaces. By using GaN barrier layer instead of InGaN barrier layer, the polarization increased at the barriers/wells interfaces leading to the appearance of the kink in the I-L curve.

(Received March 28, 2010; accepted May 26, 2010)

Keywords: InGaN, Laser diode, Barrier Thickness, Threshold current

1. Introduction

III-nitride semiconductor laser diodes (LDs) have been extensively studied and developed for high-density optical storage systems, full-color displays, chemical sensors, and medical applications. Specifically, the InGaN-based violet LDs have attracted much attention due to their application in next-generation digital versatile disc (DVD) [1,2]

A strong built-in electric field is expected in the QW due to the polarization discontinuities at the heterointerfaces. This strong electric field remarkably affects the optical properties of the InGaN QWs, such as the emission energy and the radiative lifetime [3] which in turn affects the threshold current, efficiency, and output power of the InGaN-based LDs. This built-in electric field

can be modified by the optimization of barrier type, doping, and thickness. The barrier thickness

is found to affect in determining the optical and interfacial structural qualities of the MQWs [4]. The doping of the barrier layer with heavy amount of Si is found to increase the output power and reduce the threshold current of the LDs [5] and this also leads to reducing the polarization at the heterointerfaces [6]. On the other hand, the optical properties of the blue-violet InGaN LDs can also be affected by barrier type. Recently, some investigations have turned to the use of a quaternary $Al_xIn_yGa_{1-x-y}N$ alloy as barrier layers for the InGaN QWs grown on a relaxed $In_xGa_{1-x}N$ template [7,8]. It was found that the emission properties were improved for unstrained InGaN/AlInGaN QWs on the InGaN template with suitable indium composition [9].

In this paper, the authors investigate the effects of the barrier thickness and type on the threshold current and I-L curve shape of violet InGaN LD numerically.

2. Laser diode structure and parameters

The two-dimensional **ISE TCAD** (**I**ntegrated **S**ystem **E**ngineering **T**echnology **C**omputer **A**ided **D**esign) simulation program is utilized. Carrier drift-diffusion model and Newton method are used. The ISE TCAD self-consistently solves electronic and optical equations in a quantum well laser. The carrier capture model in the quantum well is linked to the electronics and optic equations. Auger and Shockley-Read-Hall (SRH) non-radiative recombination deplete the QW carriers [10]. The electronic equations are the Poisson and the continuity equations of both free and bound electrons and holes. A scalar Helmholtz equation is used to solve the optical problem, and a photon rate equation is used to calculate the photon spectrum of each mode where the photon rate equation contains the model gain, the optical loss, and the spontaneous emission. The total optical losses are: free carrier absorption loss, cavity loss, background optical loss, and waveguide loss [10]. The electronic band structure of quantum well is calculated using k.p theory of wurtzite semiconductors [11]. Spontaneous and stimulated optical recombinations are calculated in the active region according to Fermi's golden rule. As a result, the coupling between the optical and electronic equations leads to convergent problems of the Newton method [10].

A schematic diagram of the violet InGaN laser diode structure under study is shown in Fig. 1. In this simulation, it is assumed that the InGaN laser diode is grown on the n-type GaN layer whose thickness is 2 μm. On the top of this GaN layer is a 0.1- μm-thick n-type $In_{0.05}Ga_{0.95}N$ compliance layer and a 0.48- μm-thick n-type $Al_{0.07}Ga_{0.93}N$ cladding layer, followed by a 0.1-μm-thick n-type GaN guiding layer. The active region of the

preliminary laser diode under study consists of double $In_{0.12}Ga_{0.88}N$ undoped quantum wells where the thickness of every well is 2.5 nm, and every well is sandwiched between two 5-nm-thick $In_{0.01}Ga_{0.99}N$ barriers. A 0.014 -μm-thick p-type $Al_{0.18}Ga_{0.82}N$ blocking layer is grown on top of the active region, followed by a 0.1-μm-thick p-type GaN guiding layer and a 0.48-μm-thick p-type $Al_{0.07}Ga_{0.93}N$ cladding layer. Finally, a 0.1-μm-thick p-type GaN cap layer is grown over p-type cladding layer to complete the structure. The doping concentrations of n-type and p-type are equal to $1\times10^{18}cm^{-3}$ and $5\times10^{18}cm^{-3}$ respectively. The active region is 1 μm in width and 750 μm in length. The reflectivities of the two end facets are 50% for each one.

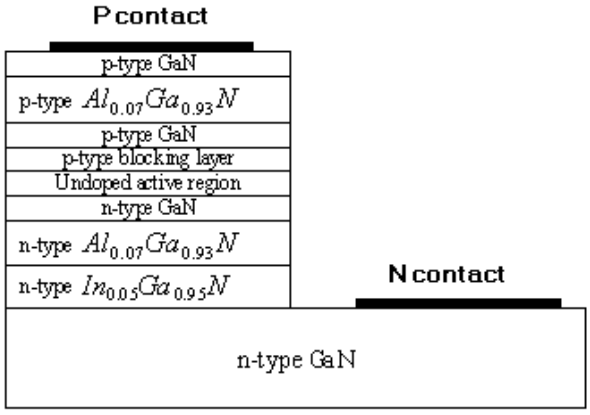

Fig. 1. The schematic diagram of violet InGaN laser diode under study.

It is assumed that the strained quantum well is grown along (0001) direction. Therefore, the strain tensor in the plane of the epitaxial growth is [12]:

$$\varepsilon_{xx} = \varepsilon_{yy} = \frac{a_o - a}{a} \tag{1}$$

Where (*a*) *is* the natural unstrained lattice constant of the quantum well and (a_o) is the lattice constant of the GaN. The perpendicular strain tensor can be obtained by the following equation [11]:

$$\varepsilon_{zz} = -\frac{2c_{13}}{c_{33}}\varepsilon_{xx} \tag{2}$$

Where (C13) and (C33) represent the elastic stiffness constants.
While:

$$\varepsilon_{xy} = \varepsilon_{yz} = \varepsilon_{zx} = 0 \tag{3}$$

The parameters required for the k.p. method calculations of the AlInGaN materials can be obtained by a linear interpolation between the parameters of the relevant binary semiconductors (Table 1). For physical parameter *P*, the interpolation formula is [12]:

$$P(Al_xIn_yGa_{1-x-y}N) = P(AlN)x + P(InN)y + P(GaN)(1-x-y) \tag{4}$$

It is evident that, when x = 0 in formula (4), the formula becomes for InGaN alloy, also when y = 0, the formula becomes for AlGaN alloy.

The refractive indices of $Al_xGa_{1-x}N$ and $In_xGa_{1-x}N$ are given by Eq. 1 and Eq. 2, respectively as [13]:

$$n(Al_xGa_{1-x}N) = 2.5067 - 0.43x \tag{1}$$

$$n(In_xGa_{1-x}N) = 2.5067 + 0.91x \tag{2}$$

The band gap energies of $Al_xGa_{1-x}N$ and $In_xGa_{1-x}N$ are given by Eq. 3 and Eq. 4, respectively as [14]:

$$E_{g,In_xGa_{1-x}N} = x\cdot E_{g,InN} + (1-x)E_{g,GaN} - 1.43\cdot x\cdot(1-x) \tag{3}$$

$$E_{g,Al_xGa_{1-x}N} = xE_{g,AlN} + (1-x)\cdot E_{g,GaN} - 1.3\cdot x\cdot(1-x) \tag{4}$$

The laser parameters which have been used in our simulation are listed in Table 1 below [15, 16,17]:

Table 1. The laser parameters which have been used in ISE TCAD simulation program

Parameter	symbol (unit)	GaN	AlN	InN
Lattice constant	a_o (A^o)	3.189	3.112	3.545
Spin-orbit split energy	Δ_{so} (A^o)	0.017	0.019	0.005
Bandgap energy	E_g (ev)	3.42	6.2	0.77
Elastic stiffness constant	C_{33} (GPa)	398	373	224
Elastic stiffness constant	C_{13} (GPa)	106	108	92
Electron effective mass	m_e (m_o)	0.2	0.4	0.11
Heavy hole effective mass	m_{hh} (m_o)	1.595	3.53	1.44
Light hole effective mass	m_{lh} (m_o)	0.26	3.53	0.157

3. Simulation results and discussion

Fig. 2 shows the diagram of the energy band gap of the LD under study. The right side of the diagram is assumed to be n-side and the left side of the diagram is assumed to be p-side of the laser structure. The horizontal axis which is entitled vertical position is assumed to be the distance along the crystal growth direction.

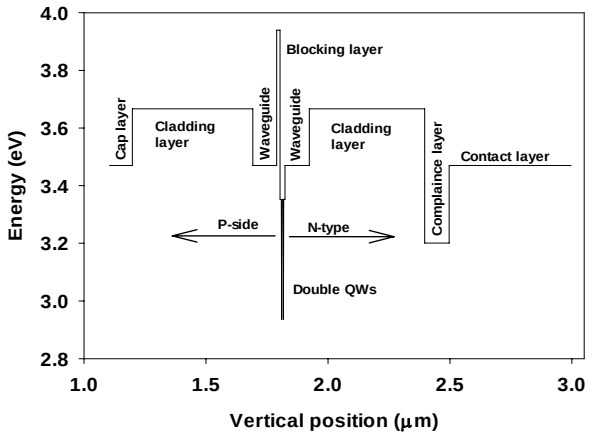

Fig. 2. The energy bandgap diagram of LD.

To investigate the effect of $In_yGa_{1-y}N$ barrier thickness on the properties of $In_xGa_{1-x}N/In_yGa_{1-y}N$ MQWs, the $In_yGa_{1-y}N$ barrier thickness is varied, while keeping the thickness of the $In_xGa_{1-x}N$ wells constant at the 2.5 nm.

Fig.3 shows $In_yGa_{1-y}N$ barrier thickness as a function of optical confinement factor (OCF) and optical intensity inside the active region. As can be seen, when the barrier thickness decreases the OCF increases. As a result, the optical intensity inside the active region increases.

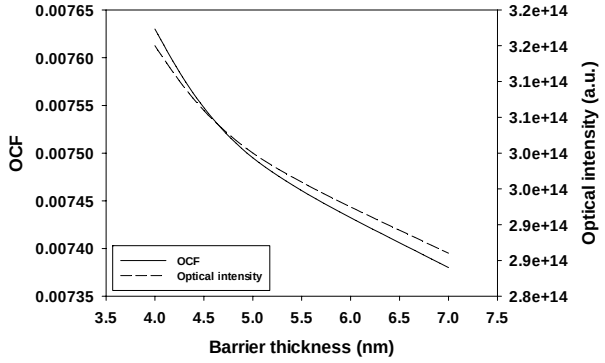

Fig.3. The OCF and optical intensity as a function of barrier thickness.

The increase in the $In_yGa_{1-y}N$ barrier thickness makes the interfaces in the MQWs rougher. This can be attributed to the deteriorating quality of the interfacial structure of the MQWs caused by the generation of defects such as threading dislocation through the partial relaxation of the strain accumulated in the $In_xGa_{1-x}N/In_yGa_{1-y}N$ MQWs [18]. Moreover, the thick barrier is not recommended experimentally as it is reported that the large defect density caused by thicker barrier layer consequently enhanced the niterdiffusion of In in the MQWs interfaces [19]. Hence, deterioration of the LDs properties with thicker barrier layer is expected.

Therefore, the radiative recombination process inside the quantum well is limited, while the non-radiative recombination increases as heat inside the structure [5]. As a results, the output power decreases while the threshold current increases when the barrier thickness is larger, as indicated in Fig. 4.

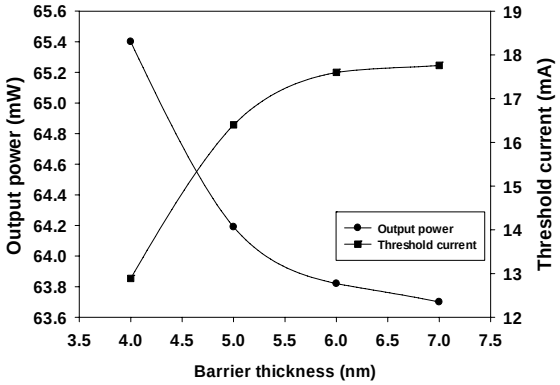

Fig. 4. Output power and threshold current of the LD versus barrier thickness.

In spite of the thinner barrier layer getting the higher output power and lower threshold current of the LD, the deep understanding of this result recommends not to consider the thinner barrier for the blue-violet InGaN LDs where the light output-current (L-I) curve of the LD with the thinner $In_yGa_{1-y}N$ barrier layer (at barrier thickness = 4 nm) is not kink-free; while the L-I curve of the LD with barrier thickness = 5 nm is kink-free and linear in the entire range, implying single transverse mode operation up to at least 60 mW, as shown in Fig. 5.

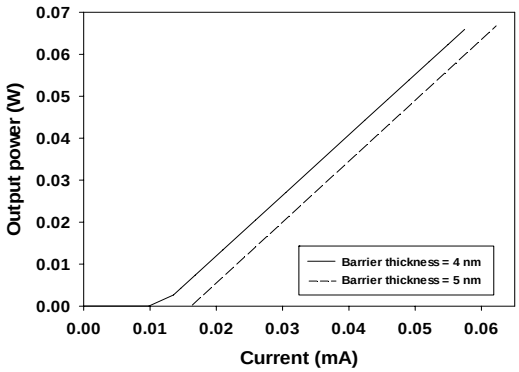

Fig. 5. L-I curves of LD with barrier thicknesses 4 and 5 nm.

Since the main purpose of the barrier layers in the MQWs active region of the LDs is to prevent coupling between adjacent wells, hence, when the thickness of the barrier layers are thin enough, the wavefunctions of electrons and holes would penetrate the adjacent well layer, resulting in the interwell transitions. This leads to increase in the piezoelectric field (20).

Consequently, it can be concluded that the kink in the L-I curve with thinner barrier layers is due to increase in the piezoelectric field at the MQWs interfaces. However, there is another evidence for the appearance of kink in the L-I curve is due to the piezoelectric field at the In_xGa_{1-}

$_x$N/In_yGa_{1-y}N MQWs interfaces. This evidence can be introduced by using GaN as a barrier layer instead of $In_yGa_{1-y}N$ barrier layers where it is well known that the lattice mismatched-induces piezoelectric field between InxGa1$_{-x}$N/GaN interfaces which is larger than the $In_xGa_{1-x}N/In_yGa_{1-y}N$ interfaces for interesting mole fractions of barriers and QWs. In this study, the specific mole fractions are assumed, x = 0.12 for QWs and y = 0.01 for barriers, i.e. the piezoelectric field at the interfaces between $In_{0.12}Ga_{0.88}N$/GaN MQWs will be larger than the piezoelectric field at the interfaces between $In_{0.12}Ga_{0.88}N/In_{0.01}Ga_{0.99}N$ MQWs because the mismatched lattice constant between $In_{0.12}Ga_{0.88}N$ QWs and GaN barriers is larger than the mismatch between $In_{0.12}Ga_{0.88}N$ QWs and $In_{0.01}Ga_{0.99}N$ barriers. Regarding our argument, the kink in L-I curve is expected to appear, considering the GaN as barrier instead of $In_{0.01}Ga_{0.99}N$ barriers in the LDs under study. This can be confirmed from Fig. 6 which represents the L-I curves of the LDs with $In_{0.12}Ga_{0.88}N/In_{0.01}Ga_{0.99}N$ and $In_{0.12}Ga_{0.88}N$/GaN MQWs with barrier thickness = 5 nm.

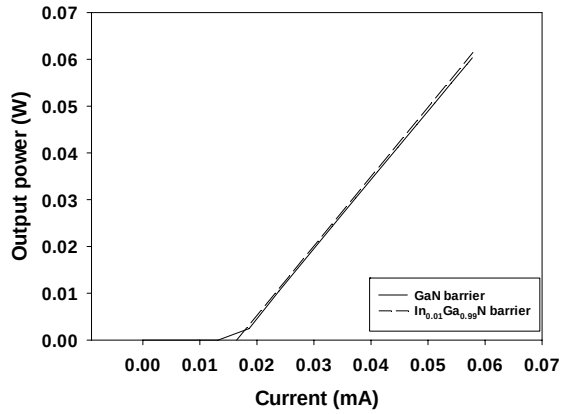

Fig. 6. The L-I curves of the LDs with $In_{0.12}Ga_{0.88}N/In_{0.01}Ga_{0.99}N$ and $In_{0.12}Ga_{0.88}N$/GaN MQWs and barrier thickness = 5 nm.

4. Conclusions

In conclusion, the optimization of the barrier thickness is important to reducing the threshold current and to increasing the output power. Simulation results indicated not to consider the thinner barrier layer in spite of the lower threshold and higher output power obtained with thinner barrier layer, but with thinner layer the polarization at the interfaces has increased. This result has been confirmed in another way, by changing the barrier type from InGaN to GaN. Simulation results suggested that the $In_{0.01}Ga_{0.99}N$ barrier layer is batter than GaN barrier.

References

[1] S. N. Lee, S. Y. Cho, H. Y. Ryu, J. K. Son, H. S. Paek, T. Sakong, T. Jang, k. K. Choi, K. H. Ha, M. H. Yang, O. H. Nam, Y. Park, Appl. Phys. Lett. **88**, 111101 (2006).
[2] Sheng-Horng Yenand Yen-Kuang Kuo Meng-Lun Tsai,Ta-Cheng Hsu, Appl. Phys. Lett. **91**, 201118 (2007).
[3] T. Takeuchi, S. Sota, M. Katsuragawa, M. Komori, H. Takeuchi, H. Amano, I. Akasaki, Jpn. J. Appl. Phys., Part 2 **36**, L382 (1997).
[4] Dong-Joon Kim, Yong-Tae Moon, Keun-Man Song, Seong-Ju Park, Jpn. J. Appl. Phys., **40**, 3085 (2001).
[5] S. M. Thahab, H. Abu Hassan, Z. Hassan, Opt. Express, **15**, 2380 (2007).
[6] G. Franssen, T. Suski, P. Perlin, R. Bohdan, A. Bercha, W. Trzeciakowski, I. Makarowa, P. Prystawko, M. Leszczyñski, I. Grzegory, S. Porowski, S. Kokenyesi, Appl. Phys. Lett., **87**, 041109 (2005).
[7] T. Takeuchi, S. Sota, M. Katsuragawa, M. Komori, H. Takeuchi, H. Amano, I. Akasaki, Jpn. J. Appl. Phys., Part 2 **36**, L382 (1997).
[8] M. E. Aumer, S. F. LeBoeuf, S. M. Bedair, M. Smith, J. Y. Lin, H. X. Jiang, Appl. Phys. Lett. **77**, 821 (2000).
[9] M. E. Aumer, S. F. LeBoeuf, B. F. Moody, S. M. Bedair, K. Nam, J. Y. Lin, H. X. Jiang, Appl. Phys. Lett. **77**, 3099 (2002).
[10] ISE TCAD user's manual release 10.0, Zurich, Switzerland, 2004.
[11] S. L. Chuang, C. S. Chang, Phys. Rev. B **54**, 2491 (1996).
[12] J. Minch, S. H. Park, T. Keating, S. L. Chuang, IEEE J. Quantum Electron. **35**, 771 (1999).
[13] H. Y.Zhang, X. H. He, Y. H. Shih, M. Schurman, Z. C. Feng, R. A. Stall, Opt. Lett. **21**, 1529 (1996).
[14] Yen-Kuang Kuo, Yi-An Chang, IEEE J. Quantum Elect., **40**, 437 (2004).
[15] V. Fiorentini, F. Bernardini, O. Ambacher, Appl., Phys., Lett., **80**, 1204 (2002).
[16] D.Fritsch, H.Schmidt, and M.Grundmann, Phys.Rev. B **67,** 235205 (2003).
[17] Michael E. Levinshtein, Sergey L. Rumyantsev, Michael S. Shur, John Wiley & Sons, Toronto, Canada, (2001).
[18] Dong-Joon Kim, Yong-Tae Moon, Keun-Man Song, Seong-Ju Park, Jap. J. Appl. Phys., **40**, 3085 (2000).
[19] Yong-Hoon Cho, J. J. Song, S. Keller, M. S. Minsky, E. Hu, U. K. Mishra, S. P. DenBaars, Appl. Phys. Lett. **73**, 1128 (1998).
[20] H. Kollmer, Jin Seo Im, S. Heppel, J. Off, F. Scholz, A. Hangleiter, Appl. Phys. Lett. **74**, 82-84 (1999).

*Corresponding author: rafid_alabdali@yahoo.com